The payloads of Advanced Virgo: current status and upgrades

IOP Conf. Series: Journal of Physics: Conf. Series **957** (2018) 012002 doi:10.1088/1742-6596/957/1/012002

The payloads of Advanced Virgo: current status and upgrades

L. Naticchioni[1,2] ***on behalf of the Virgo Collaboration***

[1]Università di Roma *Sapienza*, I-00185 Rome, Italy
[2]INFN - Sezione di Roma, I-00185 Rome, Italy

E-mail: luca.naticchioni@roma1.infn.it

Abstract. The development and integration of new detector payloads has been an important part of the Advanced Virgo (AdV) project, the major upgrade of the Virgo interferometric detector of Gravitational Waves, aiming to increase the detector sensitivity by one order of magnitude. During the integration phase of the new AdV payloads with monolithic suspension of mirrors we experienced systematic suspension failures later identified as caused by dust contamination of the vacuum system. In order to not postpone the detector commissioning, making possible to join the LIGO O2 observation run, the Collaboration decided to proceed with the integration of the payloads relying on steel wire suspensions for all the mirrors. In this proceeding the status of the currently integrated payloads is reported, including their angular control characterization and the Q-factor measurements for test mass steel wire suspensions. The payload upgrade for the re-integration of monolithic suspensions after the O2 run is reported in the last section.

1. Introduction

The first observations of gravitational waves (GW) [1, 2, 3] has been possible using large-scale Michelson interferometers (ITF) in which the variation of the light path due to passing GWs is detected as a fluctuation in the dark fringe signal. The largest ITF GW detectors built so far are the two 4 km-long LIGO observatories in USA and the 3 km-long European observatory Virgo in Italy. In these detectors the mirrors are suspended from seismic insulators in order to act as gravitational test masses. During the last years both LIGO and Virgo have been updated to their Advanced design. The Advanced Virgo [4] project (AdV) started in 2011 and was completed this year. The aim of this upgrade is the improvement of the detector sensitivity by one order of magnitude, reached using heavier mirrors and higher circulating laser power among other relevant changes. These requirements led to redesign the last suspension stage for the mirrors of AdV, referred to as payload. It is a double pendulum stage consisting of marionette, mirror (i.e. the test mass, TM), the associated suspensions and actuators. The payload is in turn suspended from the Superattenuator (SA) in a dedicated UHV chamber located at the base of the SA tower [4]. It is conceived for the compensation of the residual seismic noise and for the steering and control of the main optical components of the ITF.

In initial Virgo and Virgo+ payloads [5] the mirror was suspended from the marionette in parallel with a recoil mass, used for its actuation, thus forming a double stage branched pendulum [7]. In the current Advanced Virgo design this configuration was changed into a simple double stage suspension, where the mirror actuation is obtained using coils fixed to the

same mechanical structure that is also used for the marionette actuation, the so called Actuator Cage. This structure is fixed to the last steering filter of the SA and enfolds the payload, providing the support frame for baffles, thermal compensation elements (compensation plate and ring heater) [4] and acting also as safety frame for the suspended elements of the payload. In order to reduce the suspension thermal noise, the input and end mirrors of the ITF Fabry-Perot cavities are monolithically suspended from the marionette using four fused silica fibers for each mirror [8]. The removal of the recoil mass in Advanced Virgo payloads has the advantage of simplifying the payload structure and its local control, moreover it implies the reduction of thermal noise associated with the recoil mass suspension. On the other hand the simple double stage design reduces also the vertical and horizontal degrees of inertial damping provided by the suspension, that is however still compliant with the residual seismic noise requirements at the level of the mirror [6]. A direct comparison between the payloads of Virgo/Virgo+ and Advanced Virgo is shown in fig. 1. A technical drawing of the AdV Payload integrated with the SA suspension chain is shown in fig. 2.

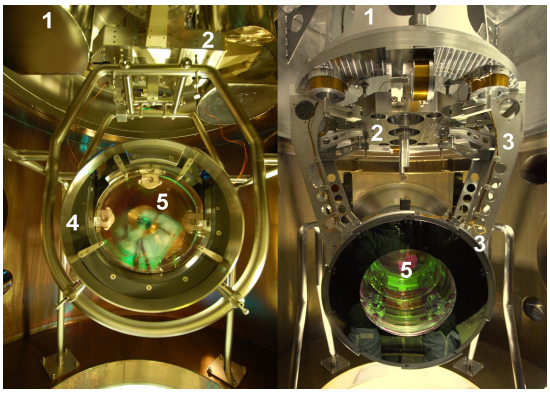

Figure 1. Comparison between Virgo+ and Advanced Virgo payloads. Main elements: 1) interface with the last SA steering filter, 2) Marionette, 3) Actuator Cage, 4) Recoil Mass, 5) Mirror.

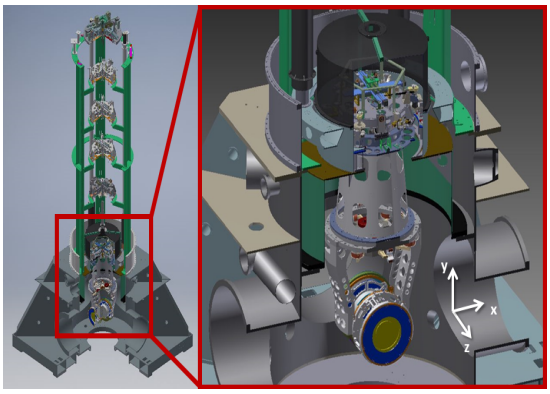

Figure 2. CAD drawings of the Advanced Virgo payload integrated in the SuperAttenuator suspension.

2. AdV Payloads in O2

Before the completion of the AdV project, seven new payloads have been integrated in Virgo: the beam splitter payload (BS), two input payloads (NI, North Input and WI, West Input), two end payloads (NE, North End and WE, West End), the Power Recycling (PR) and the Signal Recycling (SR) payloads. Even though they all share the same concept design, each type of payload is characterized by different details, as described in the next subsections. In all the payloads the marionette, suspended with a single maraging steel wire, has an octagonal shape and is made of 316L amagnetic steel plus high density copper-tungsten alloy counterweights. Moreover two counterweights can be moved along orthogonal axis by remotely controlled stepper motors, for a fine tuning of the horizontal balancing of the marionette. Input and end payloads are assembled adopting the monolithic suspension of mirrors with SiO_2 fibers [8], BS and recycling mirrors are suspended with steel wires instead. Both the pendulum stages are contained inside the Actuator Cage (fig. 3). At its top this structure has a disk-shaped element that supports the coils of the marionette actuators (coil disk in fig. 3). At both sides facing the mirror the cage is designed to support large diaphragm baffles made of stainless steel plates coated with Diamond-like Carbon that are used to reduce stray light in the main beams. The

lower part of the cage, the so called cradle, acts as a safety-stop structure for the mirror. During the integration with the SA suspension the coil disk is fixed to an interface structure that in turn is connected to the last SA steering filter (fig. 2), from which the marionette is then suspended with a steel wire. During the first vacuum operations before ITF commissioning the monolithic suspensions of input and end payloads were affected by failures, whose investigations and conclusions are given in [9]. While the tests were underway, the Collaboration decided to re-assemble input and end mirrors in their relative payloads using steel wires, in order to complete the ITF commissioning in time to join LIGO during the O2 observation run.

2.1. Beamsplitter Payload

The BS payload has been designed to host the largest mirror ever suspended in an ITF GW detector, having a diameter of 550 mm. This optical element is suspended from the marionette by four steel wires of section 300 μm. The BS payload weighs 100.5 kg and was the first to be integrated during the AdV upgrade in December 2014.

2.2. Input Payloads

The input payloads are designed for the suspension of the new AdV input test masses (ITM), that have the same diameter of initial Virgo (i.e. 350 mm), but a doubled thickness (200 mm), thus a weight of 42 kg. Considering also the marionette, the input payload weighs 145.2 kg. Their Actuator Cage (AC) is designed to host the frames and positioning mechanisms for two important elements of the thermal compensation system (TCS [4], fig. 3,4): the Compensation Plate (CP) and the Ring Heater (RH). Their fine positioning is remotely controlled by stepper motors. As in the other payload cages, the AC acts also as safety structure and support frame for marionette and mirror actuators and baffles. The AC coil disk includes a balancing mass at the opposite side of the compensation plate. Payload assembly and integration phases are shown in fig. 4.

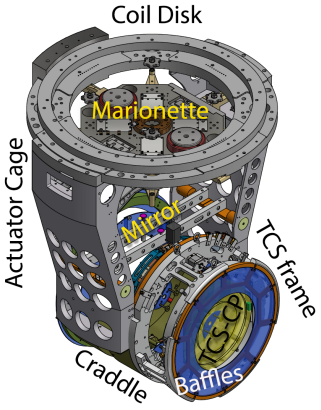

Figure 3. Input Payload, CAD drawing.

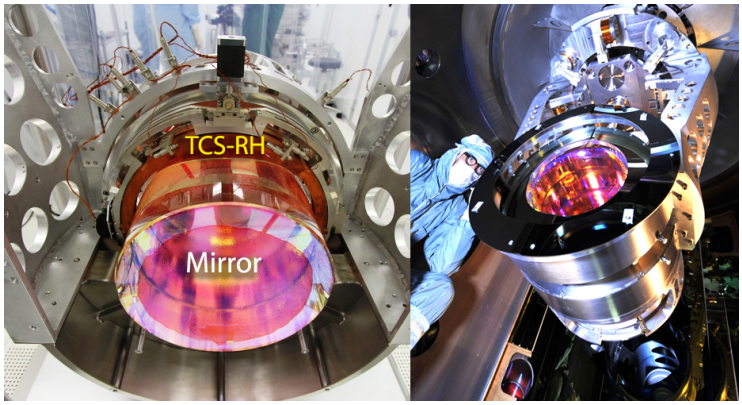

Figure 4. Input Payload during assembly (left) and its integration with SA (right).

2.3. End Payload

End payloads are similar to the input ones since the end test masses (ETM) have the same dimensions and weight (42 kg) of ITMs. Conversely their AC differs from that of input payloads, since it does not host the compensation plate support frame. However the ring heater frame and its positioning mechanism are present also in their AC.

2.4. Recycling Payloads

The power recycling (PR) and signal recycling (SR) payloads are conceptually similar to input payloads but in this case the mirrors have half the thickness and the same diameter of ITM and ETM, for a weight of 21 kg, resulting in a payload overall weight of 85.2 kg. The AC is similar to the others, providing a support frame for marionette and mirror actuators, baffles and safety stops. The cage hosts also a tilted frame for an additional optical element, the pick-off plate, used to extract the pick-off signal from the PR mirror [4]. Also the inclination of the plane of the pick-off plate with respect to the mirror can be changed by means of two stepper motors.

3. ITM and ETM payloads characterization

The angular position of the suspended payload elements (marionette and mirror) is controlled by the suspension Local Control. Given the reference frame reported in fig. 2, the error signals are produced by a set of optical levers (OpL) measuring pitch (θ_x), yaw (θ_y) and roll (θ_z) of every marionette and pitch, yaw and pendulum mode (z) of every mirror. In particular in this section we report the angular characterization of ITM and ETM payloads and the preliminary measurement of the quality factor of the current steel wire suspension.

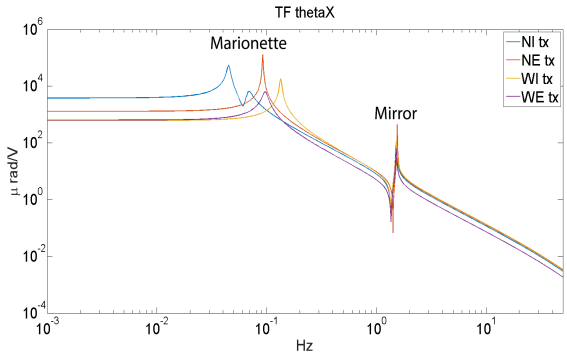

Figure 5. Pitch transfer functions for ITM (NI,WI) and ETM (NE,WE) payloads measured between marionette and mirror.

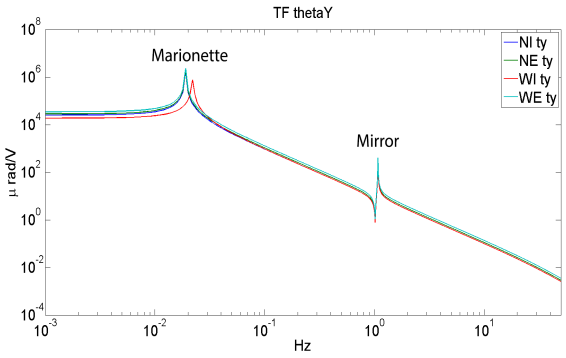

Figure 6. Yaw transfer functions for ITM (NI,WI) and ETM (NE,WE) payloads measured between marionette and mirror.

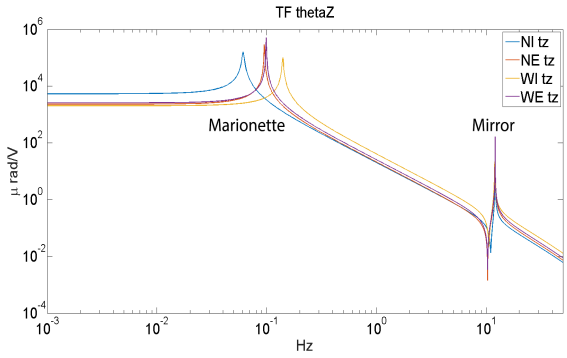

Figure 7. Roll transfer functions for ITM (NI,WI) and ETM (NE,WE) payloads measured between marionette and mirror.

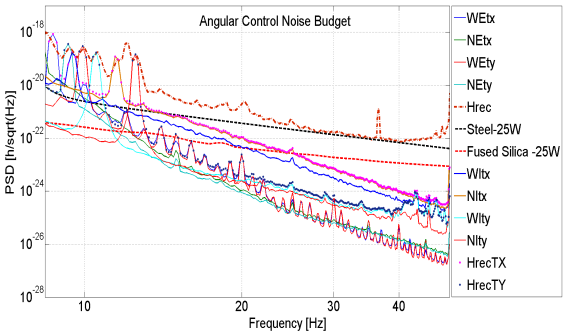

Figure 8. Angular control noise budget of TM payloads below 50 Hz, compared to dark fringe signal and target sensitivities.

3.1. Angular Transfer Functions
The angular transfer functions (TF) between marionette and mirror of each ITM and ETM payload were measured relying on the angular error signals given by the OpLs. Pitch, yaw and roll are reported respectively in fig. 5, 6 and 7. In the frequency band 300 - 800mHz the microseismic noise is transferred to the payload by the notches present in the SA transfer function and then it may impact on payload lowest modes of both pitch and roll. Therefore the payloads were designed to have those modes well below that frequency range. As choosing the backup solution of steel wire mirror suspension for the O2 run, we explored the possibility to further lowering those modes in the case of NI payload (fig. 5 and 7), successfully attaining smooth and clean operation. This feature will be adopted also during the re-integration of the monolithic suspensions.

3.2. Angular noise
Given the transfer functions between the local control and the strain (h reconstructed, i.e. the signal coming out of the ITF), the correction signal to be applied during standard operation can be easily projected, obtaining the angular noise budget reported in fig. 8. Here it is compared with the ITF target sensitivities, given a laser power of 25 W, in two cases: steel-wire suspension and monolithic TM suspension. The dark fringe signal (Hrec) achieved during the O2 run is also reported in the same figure, proving to be not limited by the angular control noises (HrecTX, HrecTY), while the spectral lines around 10 Hz are injected and demodulated to allow the ITF beam centering on the mirrors. The angular control is based upon both quadrant photodiodes (QPHD) and OpLs: a further improvement of QPHD sensors and digital filters of the control loops is foreseen after the O2 run, reducing the angular noise to allow the ITF target sensitivity.

3.3. Steel wires Q-factor
The quality factor of the steel-wire suspension of ITM and ETM was estimated injecting kicks with the motorized counterweight in the payload marionette and measuring the amplitude exponential decay of the four spectral peaks produced by the first violin mode of the wires of each payload. Indeed, the decay time τ is obtained from the exponential fit of each peak decay, and then the Q-factor is given by $Q = -\pi f \tau$. Preliminary results are given in table 1 and indicate Q-factor values ranging from 2 to 3 $\times 10^5$, in accordance with expectations for steel wires. Frequency and Q-factor ranges refer to the four wires of the single payload.

Table 1. Preliminary results of Q-factors and loss angles of the steel wire suspension of ITM and ETM in Advanced Virgo measured before O2 run.

Payload	Kick GPS time	Frequency range	Q-factor range	Loss angle ϕ
NE	1179043885	$306.6 - 314.5Hz$	$(2.21 - 2.37) \times 10^5$	$\sim 1.8 \times 10^{-3}$
NI	1179045541	$306.7 - 313.6Hz$	$(2.18 - 2.71) \times 10^5$	$\sim 1.7 \times 10^{-3}$
WI	1179047015	$307.3 - 311.8Hz$	$(2.03 - 2.69) \times 10^5$	$\sim 1.5 \times 10^{-3}$
WE	1179048159	$308.8 - 311.7Hz$	$(1.94 - 2.92) \times 10^5$	$\sim 2.0 \times 10^{-3}$

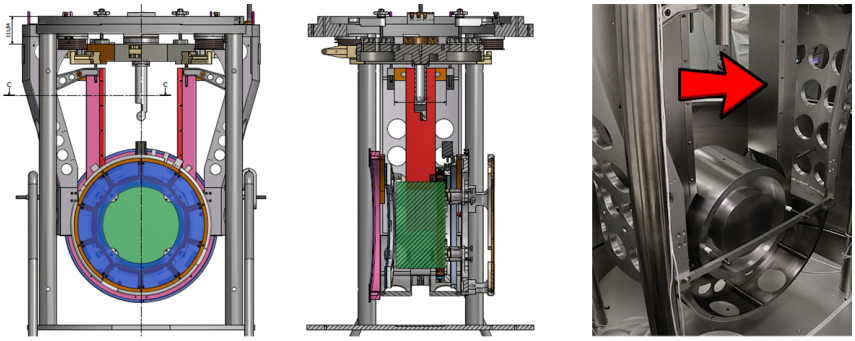

Figure 9. Test payload with monolithic suspension and FG integrated, indicated by red and purple in the CAD drawing and by the red arrow in the picture.

4. ITM and ETM payloads upgrade after O2

Before the O3 observation run, ITM and ETM payloads will be dismounted and their mirror steel-wire suspension will be replaced by the monolithic suspension. The complete procedure of payload extraction, disassembly, re-assembly with monolithic suspension and reintegration in the SA will require about three weeks for each payload. In addition to the planned improvements of vacuum system and cleaning procedures, a new component called Fiber Guard (FG, fig. 9) will be added to the payload AC to avoid any possible fused silica fiber failure due to the impact of high speed particles related to vacuum operations. FGs are made of thin Al-alloy and are designed to shield up to $\sim$ 90% of the fibers surface, to be compatible with the local control FOV and to not change significantly the overall suspended weight. FGs will be integrated in the AC immediately after the installation of fused silica fibers in the payload. Prototype FGs have been already integrated in a monolithic test payload (fig. 9). FEM simulation were produced to estimate the frequency shift of the AC resonant modes due to the introduction of FGs, obtaining a negligible change: less than 3% for modes below $250Hz$.

5. Conclusions

Advanced Virgo payloads integration started in 2014 and was concluded this year. TM payloads were re-integrated with steel wire suspensions after the monolithic suspension failures due to vacuum system contaminations [9]. Their angular transfer functions were measured as well as the angular control noise projection. As expected for steel wires, the Q-factor of ITM and ETM payloads is in the range of 2×10^5. During the stop after the O2 observation run, TM payloads will be dismounted and re-assembled with the monolithic suspension. To prevent any possible further failure due to high speed particles during vacuum operations, among other improvements of the vacuum system, fused silica fibers will be shielded by the fiber guards, a new component of the payload actuator cage. Their integration with a monolithic suspension has been already done in a test payload.

References

[1] Abbott BP et al. 2016 *Phys. Rev. Lett.* **116** 061102
[2] Abbott BP et al. 2017 *Phys. Rev. Lett.* **119** 141101
[3] Abbott BP et al. 2017 *Phys. Rev. Lett.* **119** 161101
[4] Acernese F et al. 2014 *Class. Quantum Grav.* B **32** 024001
[5] Bernardini A, et al. 1999 *Rev. Sci. Instrum.* **70** 3463
[6] Accadia T et al. 2011 *J. Low Freq. Noise V. A.* **30** 63
[7] Accadia T et al. 2012 *J. Instrum.* **7** P03012
[8] Aisa D et al. 2016 *Nucl. Instrum. Methods Phys. Res. A* **824** 644
[9] Travasso F et al. 2017, in preparation, to be published in this volume of *J. Phys. Conf. Ser.*